



Provided by the author(s) and NUI Galway in accordance with publisher policies. Please cite the published version when available.

Title	Finite element modelling of damage in superplastic forming of a titanium alloy
Author(s)	Leen, Sean B.
Publication Date	2009-12-15
Publication Information	Leen, SB,Stoyanov, M (2009) 'Finite element modelling of damage in superplastic forming of a titanium alloy'. Int J Mater Form, 2 :287-290.
Publisher	Springer Verlag
Link to publisher's version	http://dx.doi.org/10.1007/s12289-009-0569-7
Item record	http://hdl.handle.net/10379/5402
DOI	http://dx.doi.org/10.1007/s12289-009-0569-7

Downloaded 2019-11-14T13:27:19Z

Some rights reserved. For more information, please see the item record link above.



FINITE ELEMENT MODELLING OF DAMAGE IN SUPERPLASTIC FORMING OF A TITANIUM ALLOY

S B Leen^{1*}, M Stoyanov²

¹ Formerly Division of Materials, Mechanics and Structures, University of Nottingham, UK; now Dept of Mechanical and Biomedical Engineering, National University of Ireland, Galway, Ireland

² Division of Materials, Mechanics and Structures, University of Nottingham, UK

ABSTRACT: This paper describes the application of a continuum damage mechanics methodology to the prediction of failure during superplastic forming of Ti-6Al-4V. A power law constitutive relationship is employed within a geometrically non-linear finite element model of the forming process and a user subroutine is developed to implement the damage mechanics approach. The damage constants are identified from uniaxial rupture strains from constant strain-rate tests. The multiaxial implementation is successfully used to predict damage evolution during forming of a truncated cone and is shown to predict results consistent with the experimental results from forming trials.

KEYWORDS: superplastic forming, Ti-6Al-4V, damage mechanics, failure prediction.

1 INTRODUCTION

The superplastic forming (SPF) process is now widely used in a range of industries. Initially, it was developed primarily within the aerospace industry, and played a key role in high profile components such as fan blades for high by-pass gas turbine aeroengines, particularly when used with diffusion bonding (DB), to achieve high integrity bonds for internal reinforcement of blades. It is now, however, also widely used in other industries, such as the automotive industry and also in biomedical applications, e.g. for dental implants and cranioplastic implants [1]. The authors have previously presented a comparison of different failure prediction methods for SPF [2], including the flow localisation factor (FLF) approach of Chung and Cheng [3] and a novel superplastic forming limit diagram (SPFLD) approach. This paper presents a continuum damage mechanics approach for the same problem.

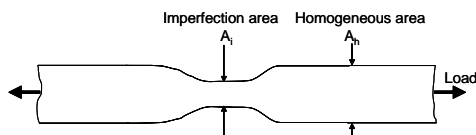


Figure 1. Assumed pre-existing geometric imperfection in tensile specimen, after Hart [4] and Ghosh [5].

2 FAILURE MODELS FOR SPF

Hart [4] presented a theory of the tensile test for rate-dependent material behaviour, using the growth of an assumed inherent inhomogeneity (Figure 1) to define the

onset of instability. Hence it was shown that the deformation is stable if:

$$\gamma \geq 1 - m \quad (1)$$

where $\gamma = \frac{1}{\sigma} \frac{d\sigma}{d\varepsilon}$ and $m = \frac{\dot{\varepsilon}}{\sigma} \frac{d\sigma}{d\dot{\varepsilon}}$ are material

parameters which vary through the deformation history in general. Hart went on to demonstrate that his model supported high ductilities for $m > 0.5$, approximately, corresponding to superplastic behaviour. Ghosh [5] further qualified the analysis of Hart and explicitly demonstrated the role of high m -values in achieving high ductility by virtue of increasing the resistance of the material to the growth of inhomogeneities and, in particular, pointed out and corrected for an error in the analysis of Hart. The latter ignored the second term in the following equation:

$$\delta\varepsilon = -\frac{\delta A}{A} + \frac{\delta A_o}{A_o} \quad (2)$$

which describes the initial imperfection (inhomogeneity) size. Ghosh has pointed out that this term is important in considering the growth or decay of any imperfection and showed that the resulting, modified version of Equation (1) was thus:

$$\gamma \geq \left[\frac{1 - m}{\left(1 - \frac{\delta \ln A_o}{\delta \ln A} \right)} \right] \quad (3)$$

so that no simple relationship exists between m and γ for instability; the initial imperfection size and the strain

* Corresponding author: s.leen@nottingham.ac.uk, Phone: 00 44 115 9513812, University Park, Nottingham, NG7 2RD, UK

history must be accounted for. More recent work on the prediction of failure during SPF deformation has been presented by Chung and Cheng [3], based on an instability criterion developed by Ding et al [6]. This was based on a thin superplastic sheet under biaxial stretching (Figure 2) and, using a procedure analogous to that of Marciniak and Kuczynski [7], analysed the conditions under which a local neck, assumed to form perpendicular to the major principal stress, σ_1 , becomes unstable. This led to the concept of a flow localisation factor (FLF) via a multiaxial generalisation of Hart's stability criterion which quantitatively predicted failure when a critical value (C_{cr}) of the integral of the FLF is achieved [8]. A key shortcoming of this and other approaches based on the Hart or even the Ghosh instability criteria is that it does not provide a means for simulating the development of the neck (imperfection or inhomogeneity); the imperfection needs to be assumed *a priori*. Furthermore, a mechanisms-based material model, e.g. Dunne and co-workers [9], which includes grain growth effects and has strain-rate independent material constants, identified from tests across a range of constant strain-rates, would be superior for identifying C_{cr} , e.g. see [10].

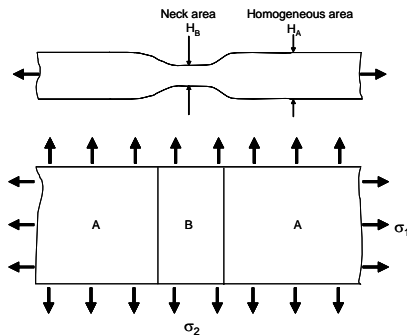


Figure 2. Assumed neck (imperfection) in biaxially stretched sheet under plane stress, after Marciniak and Kuczynski [7], Ding et al. [6] and Chung and Cheng [3].

Continuum damage mechanics (CDM) provides a framework for simulating the progressive development of material or geometric imperfections, without requiring an *a priori* assumption about the nature of this imperfection. At the same time, a CDM approach provides a basis for developing an improved SPFLD where the failure locus identification takes account of strain-rate effects more rigorously than in [10] and implicitly permits generalisation from uniaxial to multiaxial (biaxial) failure strains, in lieu of the Hill and Swift criteria (e.g. as in SPFLD), or the generalised Hart criterion (e.g. as in FLF).

3 MATERIAL AND DAMAGE MODEL

3.1 CONSTITUTIVE EQUATION

When rate effects are important, such as for superplastic deformation, then a viscoplastic constitutive equation of the following form is commonly employed :

$$\dot{\epsilon}^p = \left(\frac{\sigma}{K} \right)^m \quad (4)$$

where K and m are material constants identified as the stress axis intercept and slope, respectively, from a logarithmic plot of measured flow stress against strain rate, as obtained from constant strain-rate tests, for example. m is commonly referred to as the strain-rate sensitivity. In the present paper K and m are obtained as 7675.4 and 0.8614, respectively, from Lin et al. [11], for Ti-6Al-4V at 927 °C from flow stress data at strain rates of $1 \times 10^{-3} \text{ s}^{-1}$ and $2 \times 10^{-4} \text{ s}^{-1}$.

3.2 DAMAGE MECHANICS EQUATIONS

The damage mechanics approach adopted here is based on that used by Hyde and co-workers for creep life prediction, e.g. [12], which in turn is based on the work of Kachanov [13]. A scalar damage variable, ω , is defined as follows:

$$\omega = \frac{A_h - A_i}{A_h} = \frac{H_A - H_B}{H_A} \quad (5)$$

where A_i and A_h are defined in Fig 1 as the inhomogeneous and homogeneous load-carrying areas, respectively, and similarly for H_A and H_B in Fig 2. Thus, when the material is undamaged or for material in undamaged regions, ω has a value of zero. With increasing damage, e.g. due to deformation localisation effects such as necking, ω increases in value until failure is reached, at some critical value ω_c . In damage mechanics, a key concept is that of effective stress, σ_{eff} , which is defined as follows:

$$\sigma_{eff} = \frac{\sigma_o}{(1-\omega)} \quad (6)$$

where σ_o is the nominal stress acting on damaged load carrying area and σ_{eff} is the actual stress experienced by the damaged material due to the reduction in load-carrying area. The principle of strain equivalence [14] states that the damage effect on constitutive equations can be included by replacing the stress term in the constitutive equation by the effective stress, σ_{eff} .

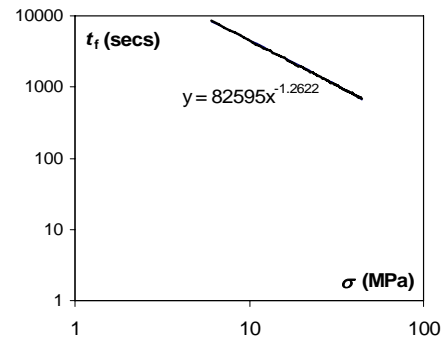


Figure 3. Stress-life rupture data for Ti-6Al-4V at 927 °C as inferred from Cope et al. [15].

Thus the modified viscoplastic constitutive equation is as follows:

$$\dot{\varepsilon}^p = \left(\frac{\sigma}{K(1-\omega)} \right)^{\frac{1}{m}} \quad (7)$$

A key aspect is the identification of an appropriate damage evolution equation, which defines the development of inhomogeneities during superplastic deformation. In this paper, which represents initial work on damage mechanics for SPF of Ti-6Al-4V here, the Kachanov damage mechanics evolution equation is investigated, as follows:

$$\dot{\omega} = M \left(\frac{\sigma}{1-\omega} \right)^{\chi} \quad (8)$$

where M and χ are material rupture constants to be determined, from uniaxial test data. The rupture constants are determined as follows.

1. Identify the uniaxial strain to failure (ε_f) for the candidate material and temperature over a range of constant strain-rates. In the present case, this data has been interpolated from Cope et al. [15], for Ti-6Al-4V at 927 °C, as previously presented in [10],
2. Identify the (approximate) steady-state flow stress, σ , for each constant strain-rate test (via Eq (4)).
3. Identify time to rupture, t_f , according to $t_f = \frac{\varepsilon_f}{\dot{\varepsilon}}$ for a given constant strain-rate.
4. Identify M and χ from σ - t_f rupture curve (Figure 3), using the integrated version of Equation (8), assuming ω_c is 1, as follows:

$$t_f = \frac{1}{M\sigma^\chi} \int_0^1 (1-\omega)^\chi d\omega = \frac{\sigma^{-\chi}}{M(1+\chi)} \quad (8)$$

5. In this case, M and χ are identified as 5.35×10^{-6} and 1.2622, respectively (units of MPa and secs).

3.3 FINITE ELEMENT IMPLEMENTATION

The multiaxial form of the coupled viscoplastic constitutive and damage evolution equations is as follows:

$$D_{ij}^p = \frac{3}{2} \left(\frac{\sigma_{eq}}{K(1-\omega)} \right)^{\frac{1}{m}} \frac{S_{ij}}{\sigma_{eq}} \quad (9)$$

$$\dot{\omega} = B \left(\frac{\sigma_{eq}}{1-\omega} \right)^{\chi} \quad (10)$$

where D_{ij}^p is the rate of plastic deformation tensor, S_{ij} is the deviatoric stress and σ_{eq} is the von Mises equivalent stress. Equations (9) and (10) have been implemented in a CREEP user subroutine in ABAQUS using explicit time integration, for large deformation, using the Jaumann rate of Cauchy stress:

$$\overset{\nabla}{\sigma} = 2GD_{ij}^e + \lambda D_{kk}^e \quad (11)$$

where D_{ij}^e is the rate of elastic deformation tensor, G is the shear modulus and λ is the Lamé elastic constant. Figure 4 shows a validation of the FE-predicted damage evolutions versus time for a constant stress uniaxial condition against the theoretical solution.

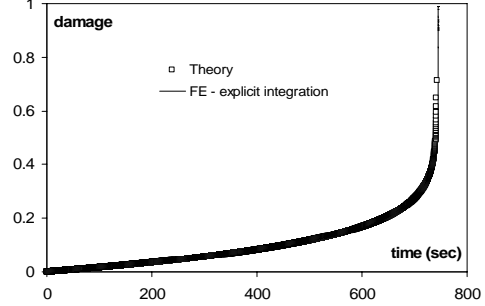


Figure 4. Validation of FE-implementation of damage mechanics against theoretical solution of damage for constant stress uniaxial condition.

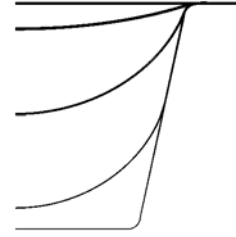


Figure 5. Predicted snapshots of truncated cone forming.

4 RESULTS

The multiaxial damage approach was investigated using a multiaxial SPF process model of an axisymmetric truncated cone, as shown in Figure 5, which has been described elsewhere [10]. Details of the SPF trials on 1 mm blank Ti-6Al-4V sheet are also given elsewhere [10]. The pressure cycle is defined utilising the FE simulation to form at a target strain-rate, as described in [2,10]. Four different target strain-rates of 0.001 s^{-1} , 0.005 s^{-1} , 0.01 s^{-1} , 0.05 s^{-1} were analysed. Figures 6 to 9 summarise the predicted damage results from the forming analyses for the different $\dot{\varepsilon}_{target}$ values.

Damage is initially uniformly distributed but with progressive forming damage begins to concentrate towards the centre (Fig 6); the final maximum damage is at $R = 20 \text{ mm}$, associated with concentrated thinning at that location, which is also evidently last to come into contact with the die (corresponding to the bottom die radius). Figure 7 shows that damage increases monotonically with strain rate, and the spatial distribution trend is effectively independent of strain-rate. Figure 8 shows that the damage rate is low initially, increases with increasing deformation before die contact but decreases after contact; Figure 9 shows the significant effect of $\dot{\varepsilon}_{target}$ on damage rate. The results of the forming trials previously presented [10], the

maximum target strain-rate value of which was 0.005 s^{-1} , showed that failure occurred for 0.005 s^{-1} , but not for lower target rates. Although the damage constants have been obtained assuming a value of ω_c of 1.0, it is clear that this value is not predicted to occur in the forming sheet for rates which gave failure. A value of 0.33 for ω_c has also been suggested for use in failure prediction, based on grain boundary failure considerations [14]; if this value was employed here, failure would be predicted first at the centre of the sheet for the 0.005 s^{-1} case, which was the observed failure location in the tests, since this location is predicted to reach higher damage levels first.

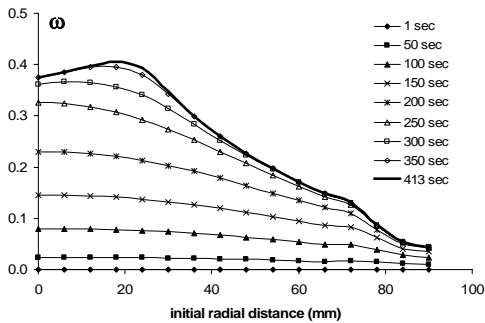


Figure 6. Snapshots of predicted damage distribution versus (initial) radial position for $\dot{\epsilon}_{t \text{ target}}$ of 0.005 s^{-1} .

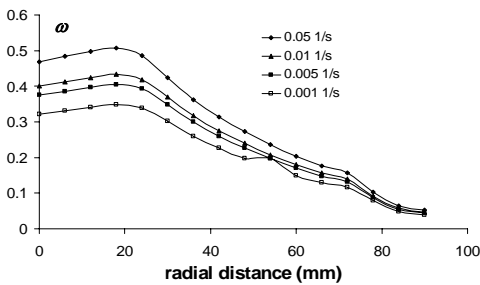


Figure 7. Predicted distributions of damage for different values of $\dot{\epsilon}_{t \text{ target}}$.

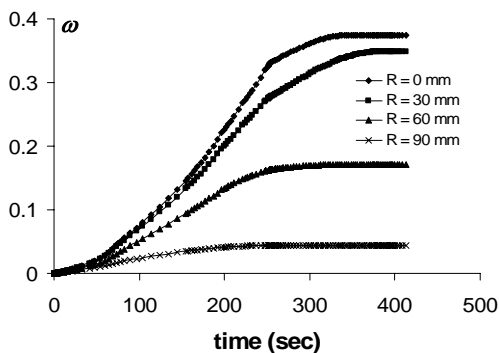


Figure 8. Predicted time-histories of damage at selected (initial) radial locations for $\dot{\epsilon}_{t \text{ target}}$ of 0.005 s^{-1} .

5 CONCLUSIONS

A damage mechanics methodology is presented for SPF of Ti-6Al-4V. The method shows promising results in

terms of correlation with forming trial results. Future work will address (i) extension to a mechanisms-based constitutive model, e.g. [16], (ii) a strain-based damage evolution equation and (iii) additional validation via more extensive forming trials. The benefit of this approach is that no *a priori* assumption about imperfections is required, as in instability methods. The method is not intended to predict cavitation, merely loss of material strength due to degradation.

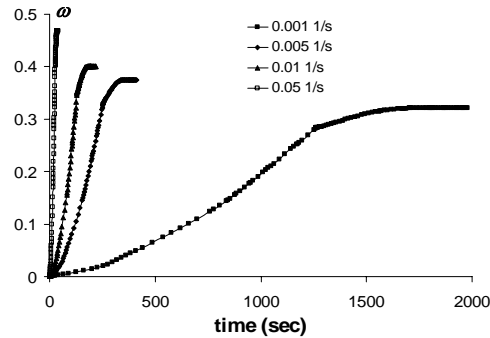


Figure 9. Predicted time-histories of damage at $R = 0 \text{ mm}$ for different values of $\dot{\epsilon}_{t \text{ target}}$.

REFERENCES

- [1] Curtis, R.V., *Mat-wiss. U. Werkstofftech.*, 39, 4-5, 2008, 309-316, DOI 10.1002/mawe.200800287.
- [2] Leen, S.B., Kröhn, M.A., Hyde, T.H., *Int. J. Mater. Form.*, DOI 10.1007/s12289-008-0205-y, Springer-ESAFORM 2008.
- [3] Chung, L.C. and Cheng, J.-H., *Mat. Sci. Eng.*, A308, 2001, pp. 153-160.
- [4] Hart, E.W. *Acta Metallurgica*, 15, 1967, pp. 351-355.
- [5] Ghosh, A.K., *Acta Metallurgica*, 25, 1977, pp. 1413-1424.
- [6] Ding, X.D., Zbib, H.M., Hamilton, C.H., Bayoumi, A.E., *Trans ASME, J Eng Mats Tech*, 119, 1997, pp. 26-31.
- [7] Marciniak, Z. and Kuczynski, K., *Int J Mech Sci*, 9, 1967, pp. 609-620.
- [8] Chung, L.C. and Cheng, J.-H., *Mat. Sci. Eng.*, A333, 2002, pp. 146-154.
- [9] Zhou, M. and Dunne, F.P.E., *J. Strain Analysis* 31, 1996, 65-73.
- [10] Kröhn, M.A., Leen, S.B., Hyde, T.H., *Proc Instn Mech. Engrs, Part L: J. Mats Design & Applications*, 221(L4), 2007, 251-264.
- [11] Lin, J., *Int J Plasticity*, 19, 2003, 469-481.
- [12] T.H. Hyde, L. Xia and A.A. Becker, *Int. J. Mech. Sci.* 38 (1996), pp. 385-403.
- [13] Kachanov, L.M., *Proc. Acad. Sci. USSR Div. Engng. Sci.* 8, 1958, pp. 26-31.
- [14] Lemaitre, J., *A Course on Damage Mechanics*, Springer, 2nd edition, Berlin Heidelberg, 1996.
- [15] Cope, M.T., Evetts, D.R. and Ridley, N., *J Materials Science*, 21(1986), 4003-4008.
- [16] Lin, J. et al., *J Mats Proc Tech*, 125-126, 2002, pp. 199-205.